



PILLARS

*Plume-deployed Inflatable for Launch and
Landing Abrasive Regolith Shielding*

Team

Abdullah Almomtan Ch '27 12	Mohammad Arbab ME '26 34	Cesar Arellano ME '25 1234	Elle Chen MS '25 234	Louise-Marie Choi-Schattle ME '27 23	Lily Coffin ME '24 1234*
Claire Ellison APh '27 12	Sam Fatemanesh Ph '27 12	Edvar Flores ME '27 1234	Sam Foxman CS '26 1234*	Ron Freeman EE '27 1	Kevin Gauld EE G1 1234*
Maria Gonzalez UD '28 34	Shan Gupta EE '27 12	Kieran Hale CNS '25 234	Noah Howell ME '26 1234	Peijuan Huang X '26 34	Noor Ibrahim ChE '27 1
Edward Ju CS '27 1	Matteo Kimura ACM '26 1234	Isabella Kwaterski ME '25 1234*	Jeylin Lee EE '27 1	Marcel Liu Ph '27 23	Fernando Matias ME '26 14
Saina Nikmehr UD '28 4	Shuban Pal X 34	Hanna Park Ph '27 1	Carmen Quinones UD '28 4	Hannah Ramsperger ME '27 1234*	Marilyn Recarte ME '24 34
Hannah Rose Ph '26 13	John Santana X '26 3	James Scott ME '26 1234*	AJ Torres ME '25 1234*	Stephanie Wallen UD '28 34	Jasmine Wang Ma '26 124
		Kenadi Waymire EE '26 1	Emily Xu EE '27 1234*		

Mentors

Dr. Charles Elachi
Caltech

Mr. Erik Franks
Cislune

Dr. Joseph Shepherd
Caltech

Advisors

Mr. Kalind Carpenter
Jet Propulsion Laboratory

Dr. Soon-Jo Chung
Caltech

- * = Team Leader
- 1 = Proposal Phase
- 2 = Design Phase
- 3 = Prototyping Phase
- 4 = Testing Phase

ACM = Applied and Computational Mathematics

APh = Applied Physics

Ch = Chemistry

ChE = Chemical Engineering

CNS = Computation and Neural Systems

CS = Computer Science

EE = Electrical Engineering

Ma = Mathematics

ME = Mechanical Energy

MS = Materials Science

Ph = Physics

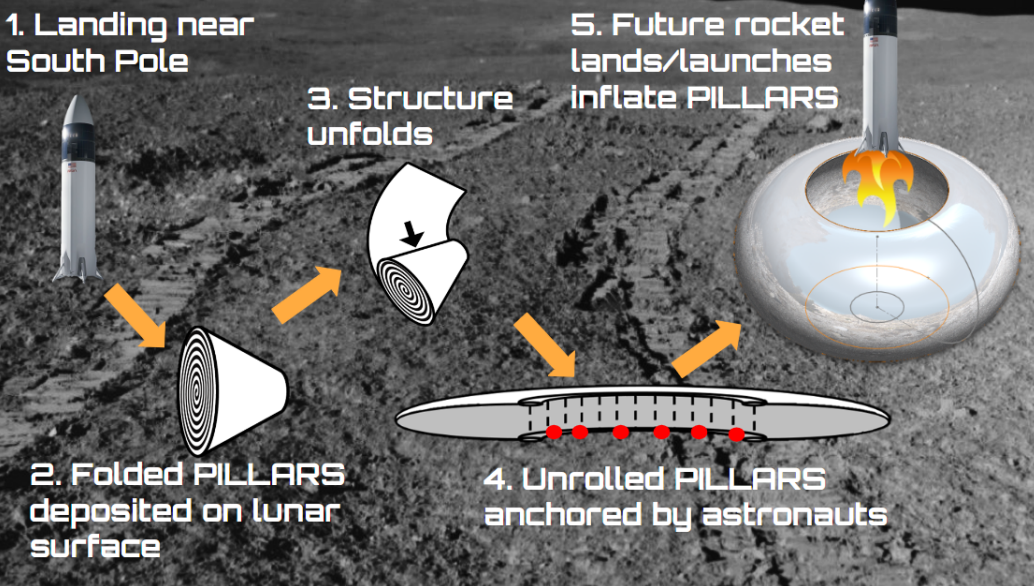
UD = Undeclared

X = Non-Caltech Student

Concept Synopsis

- PILLARS is a **Low SWaP**, inflatable solution for **dust mitigation** and containment during **launch and landing**
- Provides a **novel, lightweight** berm that **protects lunar infrastructure** in a 15km radius around the landing pad
- Uses the **rocket plume to inflate** to minimize power consumption and system complexity
- Easy to deploy** anchors for securing the structure
- High strength and durable** inflatable structure to be used as a **long-term** landing infrastructure

System CONOPS

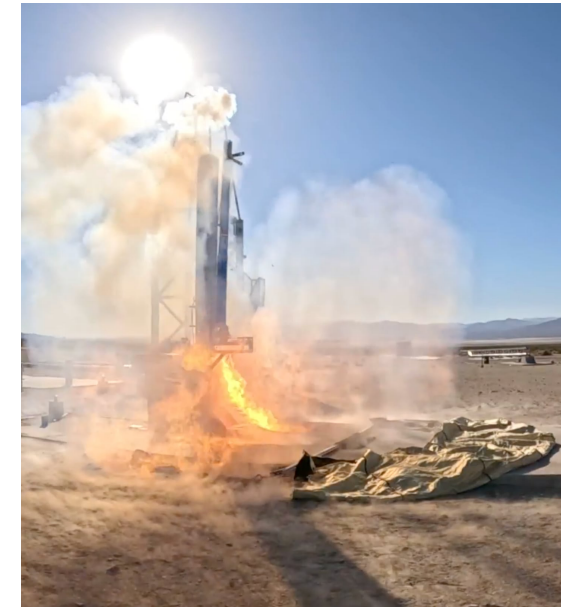


Innovations

- PILLARS is a novel **alternative to the classic landing pad** solution which bridges the gap between **early Artemis** and a **thriving lunar economy**
- Empirical data for Starship plume-surface interactions and plume expansion in vacuum **informs all Starship plume mitigation strategies**
- Advanced CFD analysis** to enforce a desired rigid shape on a membrane structure, under the influence of **high velocity flow**
- ISRU of rocket plume energy to power inflation and deflation of berm walls, ensuring **PILLARS is fully passive**

Verification Testing Results & Conclusions

- There exists an **optimal radius** for PILLARS such that the **temperature is survivable** and the **pressure is sufficient** for inflation.
- High temperature is the largest constraint** on the system and requires significant mitigation.
- PILLARS can be **scaled effectively** for **any size lander** to complement the Artemis base.



1 Executive Summary

NASA's Artemis missions aim to establish a long-term lunar habitat and thriving economy through a continuous human presence and supporting infrastructure. To achieve this, heavy-duty landers will transport humans and essential components to the lunar surface. These landings and launches will generate lunar regolith dust ejecta which will impact nearby infrastructure. The regolith particles are small, sharp, fast, and electrostatically charged, posing a threat to all lunar assets which must withstand the impact of these dust storms. Mitigating the damage caused by ejected regolith is imperative for developing permanent and sustainable lunar infrastructure.

The Plume-deployed Inflatable for Launch and Landing Abrasive Regolith Shielding (PILLARS), will prevent lunar regolith from damaging lunar bases. PILLARS is a low-mass, low-cost solution that aims to mitigate the harmful impact of rocket plumes. To withstand the impact of regolith and rocket plumes, high performance fabrics with both high tensile strength and high melting points will be utilized in construction. The structure passively inflates to a 20 meters high and 40 meters wide torus by the force of the radially-symmetric rocket exhaust during launch or landing in the center. When not in use, it automatically deflates to a nearly flat configuration. As the regolith settles, the site recovers and can be used for future launches and landings. PILLARS provides maximum mass and power savings with a stow volume orders of magnitude smaller than the deployed volume, and serves as a long term dust shielding solution for the lunar surface.

The development of PILLARS requires extensive consideration of the lunar environment and rocket plume to minimize the risk of failure. With the results of CDF simulations and experimental data, it was possible to scale PILLARS for a field demo with a 500 lbf rocket in the Mojave desert and correlate the flow parameters to be representative of the lunar scenario. Our models will allow us to scale the PILLARS system for any lunar rocket. Through our testing campaign that combines simulations, lab testing, and field demonstrations, PILLARS has been brought to a Technology Readiness Level (TRL) of 5.

Rudimentary test beds with cold air compressors, torches, and small prototypes have been constructed to validate proof of concept. Through CFD and vacuum testing, the pressure and temperature of the plume impinging on PILLARS can be understood as a function of rocket nozzle diameter, plume temperature, plume exhaust pressure, and PILLARS diameter. Inflation testing in vacuum validates the inflation mechanism and anchoring. Material abrasion testing in high abrasion and high temperature environments inform the design and construction for surviving the extreme conditions. Finally, scaled demonstrations in the Mojave desert with a bipropellant rocket prove that the models developed through our different testing campaigns provide a sufficient understanding of each aspect of the system.

PILLARS holds the potential to alleviate dust mitigation concerns for the Artemis mission, offering cost-effective shielding for early lunar bases through the use of lightweight inflatable technology. By providing efficient and deployable barriers against abrasive lunar dust, PILLARS can successfully enhance the longevity and reliability of critical equipment and habitats.

2 Problem Statement

2.1 Challenge Addressed

NASA's Artemis mission seeks to establish the infrastructure for a long-term lunar habitat and thriving lunar economy. In order to do so, it will require various heavy duty landers such as SpaceX's Starship or Blue Origin's Blue Moon lander to land payloads and astronauts on the surface of the Moon. In doing so, the rocket plumes generate dust ejecta which sends fine particles with jagged edges traveling incredibly fast [9, 4]. This causes the dust to effectively sandblast unprotected lunar infrastructure as seen with Surveyor III [2]. The concern with ejected lunar dust is so significant that the Lunar Surface Innovation Consortium (LSIC) has found that mitigation techniques are necessary to protect the future lunar outpost from the dust due to launch and landing [1]. Furthermore, LSIC analysis indicates that current proposed construction techniques for either mitigating the dust or enabling a distant landing site may need a much earlier maturation than currently anticipated to complement projected lunar activity. Although ISRU-built infrastructure is a long term goal for Artemis, there is a significant incentive for a low SWaP, intermediary system to mitigate this problem while Artemis validates and builds up its ISRU infrastructure and lunar base. As such, PILLARS seeks to fill this niche through the advantages of an inflatable system.

2.2 Mission Summary

Our solution to this destructive dust problem, PILLARS, is a 20m tall, 40m wide berm. The inflated structure will shield dust kicked up by rocket plumes on landing and launch, preventing it from reaching any nearby infrastructure. Most notably, the structure will inflate by the force of the rocket plume alone, allowing the structure to passively inflate and automatically deflate after touchdown to allow easy ingress for astronauts and transportation systems. This solution provides maximum mass and power savings, with a stow volume orders of magnitude smaller than deployed volume.

2.3 Mission Goals

Based on NASA's Moon to Mars Architecture Objectives [7] and Lunar Surface Innovation goals [6, 8], we have determined the following mission goals for our system.

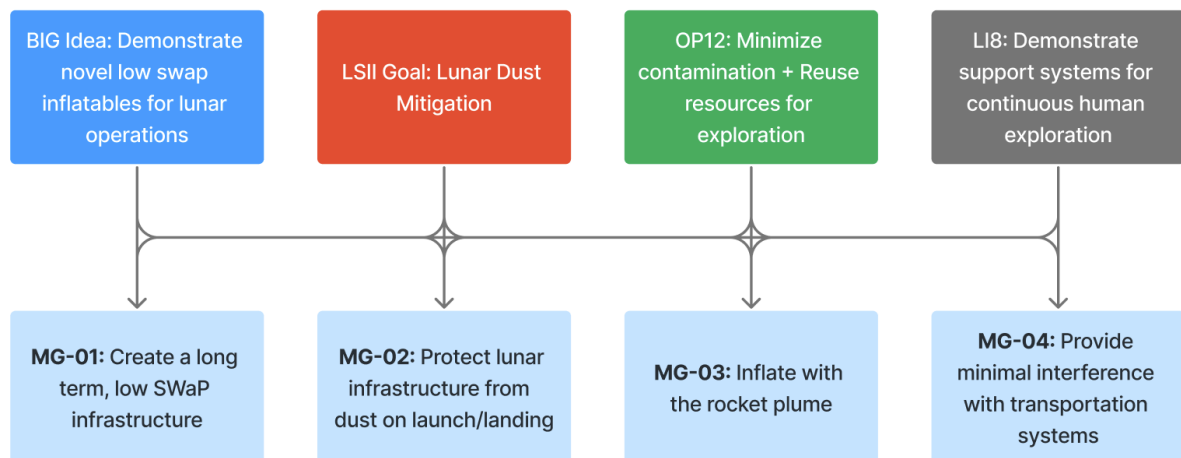


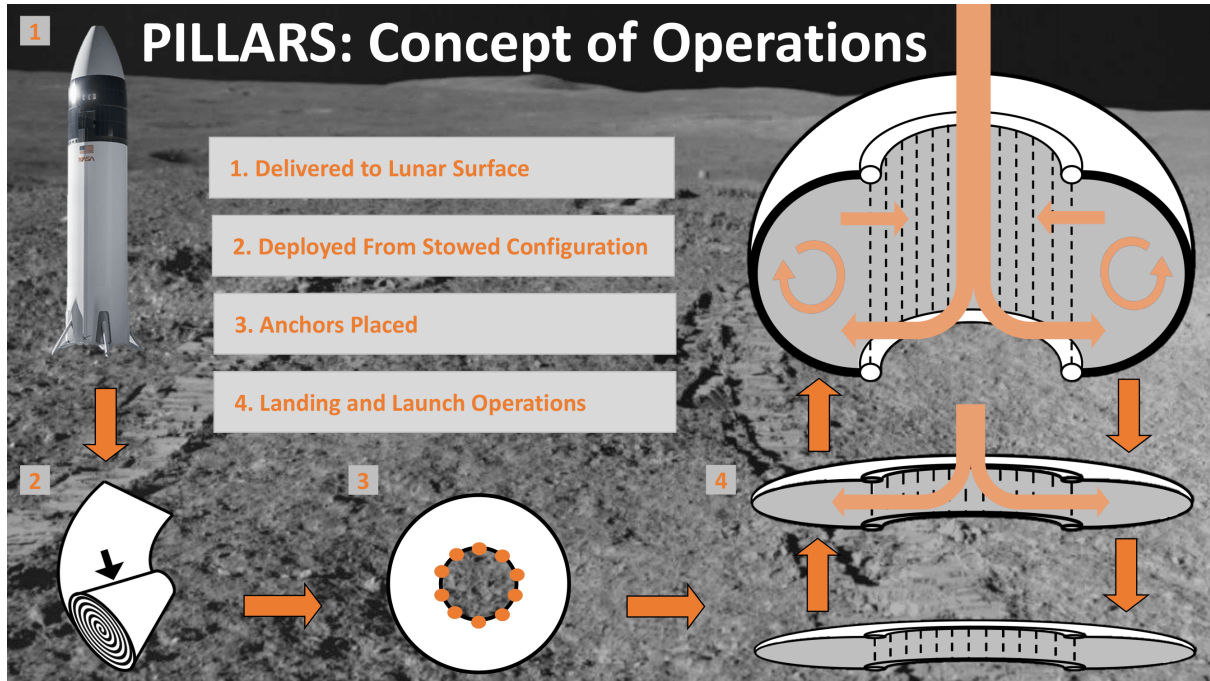
Figure 2-1

2.4 Mission Scenarios

The primary mission scenario for the usage of PILLARS is to protect the lunar base and infrastructure from landers during the early phases of Artemis while more complex surface and landing architecture is still being verified, developed, and scaled. This fills an important niche in launch and landing technologies as other proposed solutions [3, 10, 5] often trade between ambitious construction/surface preparation, complex modifications to landing architecture, short lifespan, and high maintenance. Furthermore, this system can be coupled with a landing pad or surface preparation technologies as a means to provide additional mitigation. Due to the

critical nature of landing large payloads for Artemis, PILLARS is essential for exploration and commercial operations on the Moon.

2.5 System ConOps



3 Project Description

3.1 System Specifications

PILLARS is a simple, toroidal membrane structure that is designed to withstand the extreme conditions of direct rocket fire and regolith blasting. The shield is deployed autonomously by a single-use skeletal bladder inflation, and then performs shielding operations passively. Unlike traditional berm solutions, PILLARS lays flat once the plume dissipates, providing easy cargo access. Minimal implementation complexity and cost compared to other solutions makes this robust solution significantly more feasible for enabling early infrastructure development. Starship is projected to be the primary carrier of large cargo to the lunar surface in the long term, and as the largest proposed landing system, it also poses the greatest risk to surface infrastructure. To that end, Starship is used as a model for the majority of analysis in the context of this paper. The PILLARS system is highly scalable to lunar rockets of all shapes and sizes, which puts PILLARS in a position to adapt to any developments in lunar infrastructure in the future.

Lander	Company	Lander Mass	PILLARS Mass
Starship	SpaceX	100 Tons	1,800-7,200 kg
Blue Moon	Blue Origin	21 Tons	350 - 1500 kg
Peregrine	Astrobotic	1.2 Tons	20 - 80 kg
Apollo	NASA	15 Tons	270 - 1080 kg

System Parameter	Inner Diameter	Outer Diameter	Height	Stowed Volume	Deployed Volume	Mass
Estimated Range	20 - 40 m	40 - 80 m	20 - 40 m	1.5 - 4.5 m ³	20,000 - 160,000 m ³	1,800 - 7,200 kg

for system with layer of kevlar + layer of carbon fiber

$$\text{Mass} = 2\pi R^2 * \sum_n t_n \rho_n$$

Figure 3-2

3.2 Characterizing Plume-Structure Interactions

Our challenge in developing PILLARS is understanding the expected pressure and temperature load on the shield as a result of a direct rocket plume impingement, so that a shield can be designed to operate effectively in these extreme conditions. Tools in Computational Fluid Dynamics (CFD) can be utilized in this application, however, this particular problem has proven quite extraordinary.

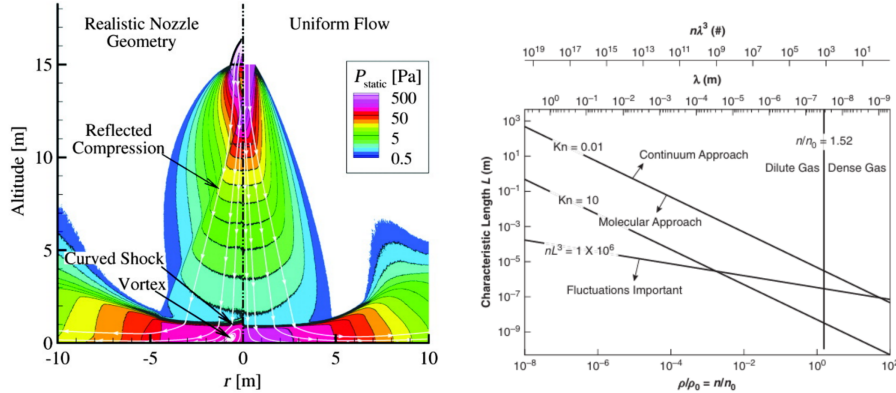


Figure 3-3: Left- Lunar rocket plume surface impingement pressures from Morris 2015. Right- Demonstrates the relationship between Knudsen number and flow regime from Boyd and Swartzentruber

A rocket that is landing or launching on the moon will exhibit the characteristic plume flow shape pictured above, where high pressure and temperature exhaust exits the rocket nozzle and quickly expands into vacuum because there is no atmosphere on the moon. When the lander is near the surface, the expanded plume will reach the solid lunar surface and stagnate—quickly condensing to high pressure once more. After stagnation, the plume will spread out radially and eventually dissipate completely. If the rocket is landing inside of a radial wall such as PILLARS, the expanding plume will stagnate a second time at the shield walls. The high pressure regions of the rocket plume are of the continuum regime, and the low pressure regions are of the molecular regime. Continuum flows are best modeled by the Navier-Stokes equations, often using standard solvers such as Ansys Fluent. Molecular flows do not obey the continuum assumption, and can only be accurately modeled as individual particle collisions in Direct Simulation Monte Carlo (DSMC). To produce an accurate simulation of PILLARS, we would have to chain five different simulations alternating between continuum and molecular flows. This approach is infeasible for the scope of this project. Given that Ansys was the most accessible tool for conducting a large number of simulations, we elected to utilize Ansys for iterating on shield design. To quantify the error imposed by a false continuum assumption, scaled down rocket tests in vacuum were performed and compared directly to simulation data. The goal was to induce rarefied flow by creating extreme pressure ratios that would force supersonic flow into a vacuum environment of 90 mtorr. This was done by igniting methane-oxygen mixtures at different pressures, and driving the explosions through a nozzle geometry.

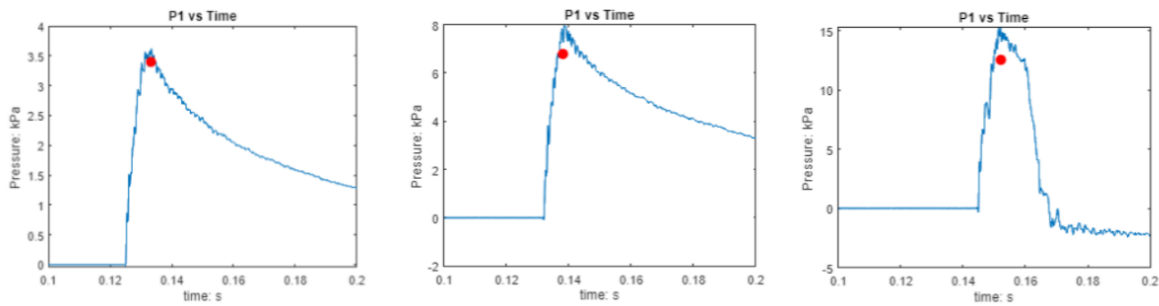


Figure 3-4: Left- Center transducer pressure versus time for the 15 bar explosion. Middle- Center transducer pressure versus time for the 30 bar explosion. Right- Center transducer pressure versus time for the 60 bar explosion. The red points are the simulated peak pressures.

For the first test, an inlet pressure of approximately 15 bar was produced, and the rocket blowdown pressure peaked at 3.616 kPa in the center of the stagnation plate. The simulation showed a very similar pressure to the test, at 3.394 kPa. The reason for this was likely that the pressure is not yet rarefied at the 15 bar / 100 mtorr pressure ratio, so the error in this case was 6.13%. The second test showed a doubling in the peak pressure, and the simulations stopped converging.

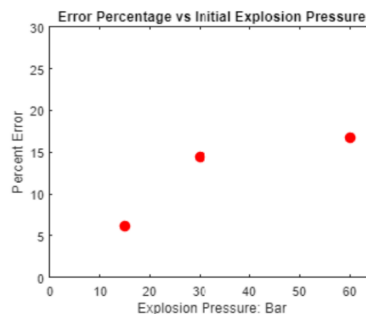


Figure 3-5: Error percentage as explosion pressure increases.

The simulation was run with increasing ambient pressures until convergence, and the peak pressure at the center location corresponding to the transducer was probed. The errors are seen in figure xxx and xxxx. These errors would likely increase for larger-scale systems.

3.3 Material Selection

The choice of material for PILLARS must consider the various environmental and technical challenges. The material needs to withstand the ambient lunar temperature range and radiation environment, high plume temperature and velocity, and high-velocity impacts of sharp regolith and micrometeoroids. It must be stiff enough to maintain the shape of PILLARS when inflated, but also be lightweight to maintain the low-SWaP nature of PILLARS. Based on these requirements, we have concluded that the material must have high tensile strength, a medium elastic modulus, high thermal resistance, and low density in order to be suitable for this application. As such, Kevlar presented itself as a strong candidate for our inflatable material.

Material	Tensile Modulus (GPa)	Tensile Strength (GPa)	UV Resistance	Thermal Resistance	Coefficient of Thermal Expansion ($10^{-6}/K$)	Density (g/cm ³)
Nextel 312	150	1.63	Excellent	Excellent	3	2.8
Aluminized Kapton Kevlar	112.4	3.6	Excellent	Great	-4.86	1.44
Kevlar 49	112.4	3.6	Poor	Great	-4.86	1.44
Carbon Fiber	231	4.5	Excellent	Excellent	1.5	1.79
Nylon	2.93	0.079	Poor	Poor	9.9	1.15

Figure 3-6: Material Selection Tradespace

However, Kevlar degrades rapidly in the presence of UV radiation. Given that the lunar environment has radiation peaks two hundred times that of Earth [11], Kevlar alone is not sufficient. Instead, PILLARS will be constructed with Aluminized Kapton Kevlar, which is Kevlar sandwiched between layers of aluminized Kapton, bolstering it against radiation. Simulation and testing has shown that Kevlar will not retain sufficient tensile strength at the expected temperature range, and in some cases will reach its melting point. Adding a layer of carbon fiber felt on the inside of the torus has proven to effectively mitigate heat transfer to the kevlar, allowing PILLARS to withstand plume impingement.

For constructing prototypes, we investigated the physical properties of Kevlar 49, Nextel 312, carbon fiber, and nylon. Being the most cost-effective, nylon was used for the creation of small preliminary prototypes, which did not require high temperature or tensile load capability. For hot fire prototyping, Kevlar 49 was chosen as a structural layer for its high tensile modulus, and higher elastic modulus. It was additionally chosen due to its cost-effectiveness and accessibility, which Nextel 312 lacked. Following initial testing, an inner carbon fiber felt layer was added to larger scale models for added temperature resistance. Additionally, the seal of our inflatable layers must be able to withstand the high temperatures that our inflatable may potentially be exposed to. In these high-temperature conditions, traditional epoxies and adhesives may fail [2], and so stitching layers together with Kevlar thread presents itself as the best option.

3.4 Berm Shape

As part of this study, we have conducted various simulations to balance the tradeoff between decreasing the system radius to guarantee inflation versus increasing the system to reduce the thermal stresses. Using Ansys simulations of a representative geometry, we ran various simulations at different rocket heights and radii to see the pressure and temperatures on a kevlar structure. To determine a baseline, we did a visual analysis of the Starship Flight 5 landing and Blue Origin BE-7 static fire (which should provide a rough estimate of a descent profile of the ship), we estimate that the duration of time interacting with the rocket plume is

around 10 seconds starting at a height of atleast 20 m. Given the wide search space we were able to quickly find a baseline shape that is 22.5 m in radius that resulted in a 17.87 time constant at a 6m rocket nozzle height. Note that these simulations are preliminary, but provide large margins for baseline.

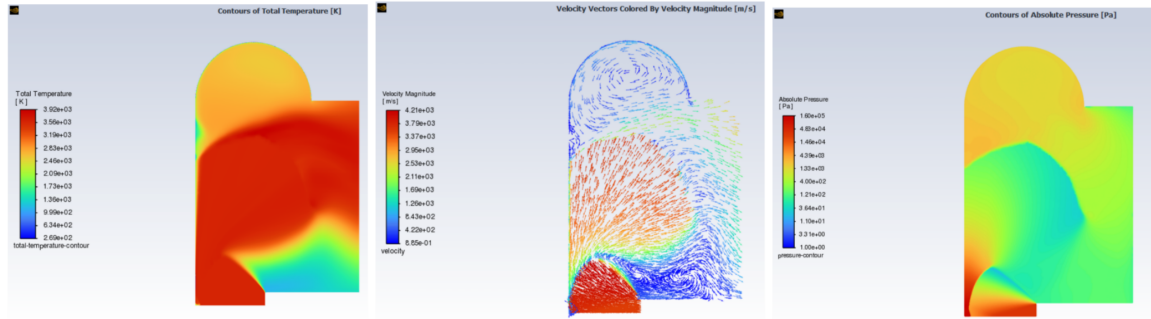


Figure 3-7: Left - Simulated Temperatures around the berm geometry, Center- Flow Velocity Vectors in the berm geometry, Right Simulated pressures aroudn the berm geometry

3.5 Manufacturing

PILLARS is a problem in fabric construction. Pulling on knowledge of garment construction, we found that the method manufacturing the PILLARS inflatable is defined by three elements: patterning, seam type, and stitch type. Construction in fabrics begins with determining how to turn a desired 3D shape into 2D panels, which can be assembled into the 3D shape. These 2D shapes are our pattern pieces. Once these pieces have been cut from fabric, we next have to think about how to attach them together. The overlap where two panels meet is a seam. To create a seam, an extra amount of fabric called a seam allowance must be cut around our pattern shape. With this extra fabric, the edges can be overlapped in multiple different ways, known as seam types. Different seam types have different uses in garment construction, impacting the durability and flexibility of a constructed design. Finally, when thread is put through fabric, such as in the creation of a seam, this known as stitching. Stitching pattern, width, and length can be manipulated, impacting the strength of construction and the behavior of the material during system use.

3.5.1 Patterning

For this project, the 3D shape of PILLARS is a toroidal shape, six meters in outer diameter, three meters in inner diameter, and one meter in height. To construct this shape, we needed to derive the dimensions of the necessary pattern pieces. However, calculating the exact dimensions and curvatures of a pattern panel by hand can be inefficient and time-intensive. To create a pattern, we instead began by modeling the exact shape in SolidWorks. With the dimensions set, the shape is exported to a Blender file. Within Blender, there exists an add-on called Seams to Sewing Pattern; this allows us to mesh our shape and define seam locations in three dimensions. We then can split the 3D object into identical 2D panels, having the computer calculate the exact shape. Once this is achieved, the 2D panel shape can be exported into any .svg file editor; for the PILLARS project, Inkscape was used. The .svg file can then be scaled to the necessary panel size given the desired dimensions.

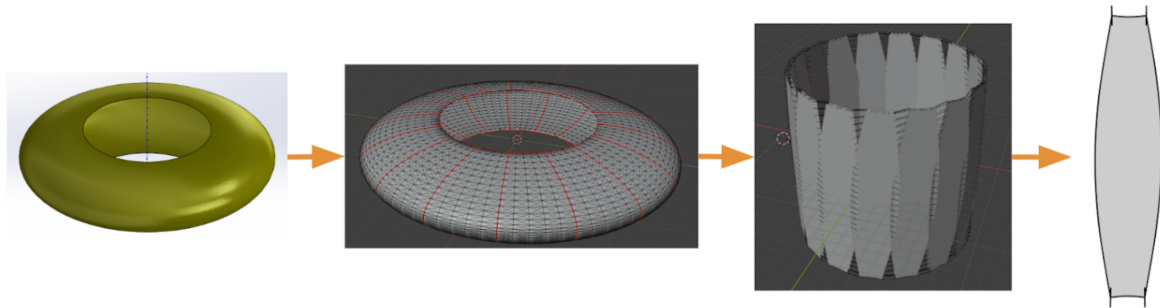


Figure 3-8: Step-by-step process of creating a pattern file. From left to right, we begin by modeling the shape in SolidWorks. The shape is split apart in Blender, with seams at the red lines. The 3D shape is blown apart into 2D panels. This 2D shape is then exported to an svg editing software for scaling and formatting.

From our Blender model, we note the number of panels required for a full model. Given the desired outer radius, we can calculate the outer circumference of model and divide by the number of panels required this will give us the width of a standard panel at its widest point. Within the svg editor, we can lock the proportions of the 2D shape, and then set the width of the shape at its widest point to equal this calculated value. This gives us an accurately scaled panel. The svg editor was also used to break large-sized panels into smaller pattern pieces. This allowed us to more compactly lay out our pattern pieces on the fabric rolls, conserving material and budget.

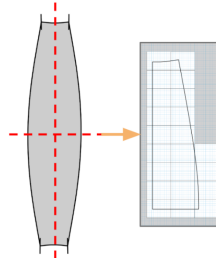


Figure 3-9: Using Inkscape, the full panel shape was divided into four identical quarter-panels, as seen on the right. This finalized pattern shape was then distributed across 22 sheets of 8.5" by 11" paper.

When the desired shape was achieved for the pattern piece, the shape could be split across standard 8.5"x11" sheets, allowing the pattern to be printed and assembled. It is important to note that the shape printed does not include a seam allowance for construction. Once printed and assembled, the pattern is cut 1" from the printed line for the entire shape. This adds extra material to account for the necessary seam allowance.

3.5.2 Seam Selection

In a typical use case, PILLARS will undergo high forces upon inflation. These forces primarily distribute along the seams of the model, so choosing a high-strength seam finish was critical to the design. Of many investigated seam finishes, we chose to use a flat-felled seam, which performed well under basic tension tests. Flat-felled seams also known to be typically used in heavy-duty garment construction.

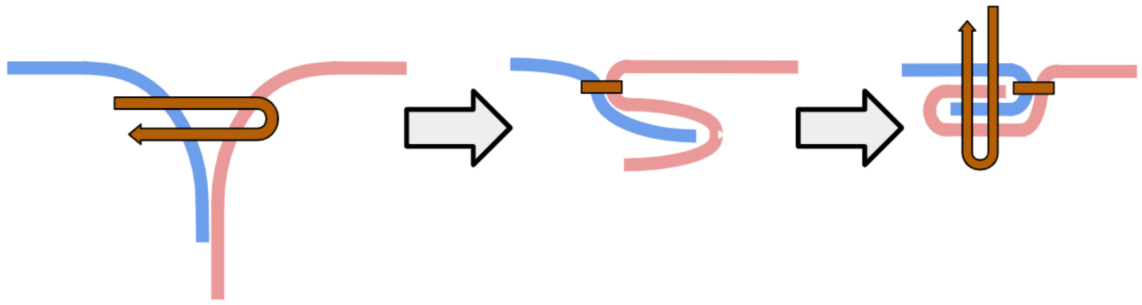


Figure 3-10: Step-by-step method of creating a flat-felled seam. The blue and pink represent the two fabric pieces to be connected, while the orange represents where stitching is done. First, the two panels will be stitched together in a basic seam, with one of the two panels having a slightly larger seam allowance. Once stitched together, the seam allowance is folded as shown, and then stitching is sewn through the folded layers.

3.5.3 Stitching

To select the best stitch type to use, we had to consider the behavior of the weave of our material. For the purpose of prototyping, plain weave Kevlar with a tow of 3000 was selected. That is, per each woven strand of Kevlar, there are 3000 fibers of the material. This means that the woven strands in our construction material are large, about 17 rows, or picks, per inch of weave. This results in a looser, more unstable weave; the picks can slide apart with minimal force, creating large gaps in the material which could allow regolith to escape shielding.

When working with this Kevlar, we needed to select a stitch type that would bind multiple picks together, stabilizing the weave. Additionally, we wanted a stitch type which could cushion impact of inflation; the stitching in the PILLARS seams needed to evenly distribute the force concentrated at the seam. After testing multiple stitch types, it was decided a plain zig-zag stitch would be the most effective choice for assembly. The peaks of the zig-zag, when set to a high stitch width, can span across approximately four picks per stitch. It was noted that under tension, zig-zag stitches could be slightly manipulated in width, expanding as the fabric stretched. This means that while the picks are bound together preventing gapping, the fabric and stitching can be flexible to inflation conditions and absorb the shock of impacts and initial inflation.

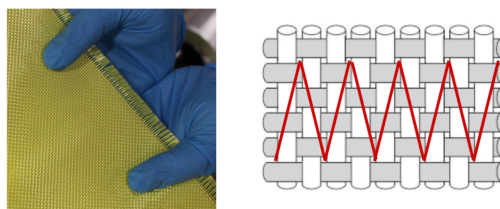


Figure 3-11: Left: An example of the loose-weave 3k tow Kevlar fabric used for prototyping. Right: A diagram of a plain weave fabric sample, with wide-width, short-length zig-zag stitches running through it. Note how the stitches cover multiple rows, or picks, of the weave, binding these rows together.

Machine stitching is done using two threads, which interlock at the end of every stitch. When under tension, the force through the stitching is distributed to the fabric at each of these interlocking points. The shorter the stitch length is, the more interlocking points you will have in the stitching. This will result in less force distributed into the fabrics at each of these interlocking points and a more even distribution of the force. To reduce the risk of the fabric failing at the seam stitching, it was decided that a small stitch length of approximately two and a half millimeters would be used.

After the first FAR test, we determined that employing these stitching choices at only the seams would not suffice for stabilizing the fabric. Impacts towards the center of a panel still

resulted in weave warping, although minimized. Seams underwent partial to complete failure in places, indicating the distribution of force from the seam to the fabric was not sufficient. Expanding on these stitching decisions and considerations, we decided that cross-stitching panels would be necessary. For each panel, several lines of zig-zag stitching would be sewn at a 45 degree angle to the direction of the weave picks. At a 45 degree angle, we were able to maximize the number of picks bound together by each cross-stitching line sewn, maximizing strength and stability. Depending on the spacing of the cross-stitching lines, a singular pick could potentially be bound in place by multiple lines of cross-stitching.

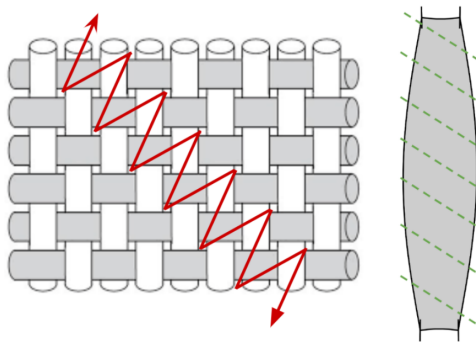


Figure 3-12: A diagram of a plain weave fabric sample, with cross-stitching sewn through it. Notice that the red zig-zag stitching now binds together a greater number of picks due to its angle respective to the weave. Cross-stitching is done for every full panel, evenly spaced across the panel as shown by the green lines on the right.

The cross-stitching lines intentionally intersect with the seams in each panel, as well as the connection seams between panels. These intersections reduce the concentration of force at the interlocking stitching points by adding even more of these interlocking points, across the entire area of the fabric panel, through which force can be distributed.

3.5.4 Internal Anchoring

In initial prototypes of PILLARS, we discovered during inflation the model did not stably hold the intended shape. As inflow fluctuated, the inner edges, corresponding to the inner diameter dimension, danced around each other in positioning and never stably aligned. This meant that the model would not inflate in a known way, and any potential rockets could get caught in or land on top of the shield. To solve this issue, we added vertical internal anchoring strips evenly spaced around the inner circumference. These strips connected the top and bottom edges of the inflatable, forcing alignment and resulting in a much more consistent inflation shape.

The internal anchoring strips can be expected to undergo a large amount of force during inflation, just like the rest of the model. However, the connection point between the anchor and the model is much smaller than any other connection point in the model. Therefore, the internal anchors needed to be incredibly robust to withstand concentrated force at the connection points. For each internal anchor, 2" by 0.5 meter strips of Kevlar and carbon fiber were cut. A carbon fiber lining was layered in between two Kevlar pieces. These three layers were sewn together along the two sides of the long dimension using the chosen stitching type, and then densely cross-stitched at two different angles.



Figure 3-13: Left: A partially completed internal anchor. The three layers are sewn together, and cross-stitching is being sewn in 1" intervals. Right: A completed internal anchor, with bi-directional cross-stitching. The internal anchor is affixed to the PILLARS inflatable along the inner circumference edge finish.

3.5.5 Anchoring Interface

One of the highest-stress areas of the model is at the interface between model and the anchors. Connecting an anchor results in a high stress concentration at the point of connection during inflation. This must be distributed to prevent failure at the anchoring point. To accomplish this, a large, heavy-duty “patch” was designed to bear the bulk of stress at the attachment point, and then distribute it over a large area of the fabric model. These patches, like the internal anchors, consist of a carbon fiber lining layered between two Kevlar pieces. The three layers were attached together and then cross-stitched for maximum strength.

Holes must be cut into this patch to attach the anchor. For the purpose of this project, we primarily used carabiner and screw attachments. These holes needed to be heavily reinforced, given that maximum stress will concentrate at this attachment point. Dense zig-zag stitching was used to create a strong, interlocked edge finish for each hole. This was reinforced using brass press-grommets, which minimize the likelihood of this stitching unraveling. It is important to note that the brass grommets themselves, when tested, could not prevent the weave from unraveling, and only assisted the anchors in ripping through the model fabric; therefore, the edge-finishing stitching around the hole was critical for the patch to function properly.



Figure 3-14: A nearly completed anchoring interface patch. Three layers are sewn together, with bi-directional cross-stitching. Dense stitching can be seen at the central connection hole acting as an edge finish. The bottom of the brass grommet has been placed in the center hole, and only the top of the grommet needs to be connected for a finished anchoring interface patch.

Once created, the patch can be sewn directly onto the model. The patch is sewn on along its main edges, and then reinforced by stitching along the patch’s cross-stitching to connect to the full model. The final anchoring interface patch was approximately 8" by 8", meaning that

the attachment distributes the force applied by the anchor across 64 square inches, compared to the half-inch size of a single grommet.

3.5.6 Assembly

With the pattern, seam type, and stitching type selected, we now have enough information for construction to begin on a prototype. Construction began with the creation of individual panels. For a 17-panel toroidal shape, 68 quarter-panels are cut from Kevlar and connected to create the Kevlar layer. From hot fire testing and the first FAR test, we learned that Kevlar, though high in strength, was not optimal for withstanding the heat of the rocket plume. We determined the carbon fiber felt could be used as an effective thermal lining, protecting the Kevlar from degrading. Carbon fiber felt does not have a high yield strength, however, so a Kevlar exoskeleton would still be necessary. Therefore, in addition to the Kevlar panels, 68 more quarter-panels must be cut from carbon fiber felt and connected to form whole panels.

With full panels of Kevlar and carbon fiber assembled, each full panel of Kevlar is connected to a lining panel of carbon fiber felt. When working with large sewing projects, keeping the material aligned can be especially tricky; attaching the lining to the exterior in this step allows for easier sewing in future steps by ensuring the lining and exterior stay aligned. To finish each full panel, cross-stitching is sewn through the layered carbon fiber and Kevlar. During the FAR test it was additionally noted that the carbon fiber felt would shred under impact and tension. In the case of a failure, cross-stitching through the carbon fiber as well as the Kevlar will ensure all tension is distributed to the Kevlar and will minimize the propagation of any tears in the carbon fiber.

With the panels completed, they are ready for connection. The panels are connected along their long edges first. Once the full body of PILLARS is connected together, the top and bottom inner edges are finished with a basic double-fold-over edge finish. This prevents the panel connections from starting to fail at the top and bottom edges. As this double-fold edge finish is created, internal anchoring strips are tucked and sewn into the folds at evenly spaced positions, connecting the top and bottom inner edges. Finally, the anchoring interfaces sewn on as necessary for the anchoring set-up.

3.6 Anchoring

PILLARS will undergo initial deployment on the Moon within a flat area for Starship to land and deploy PILLARS safely. The deployment mechanism involves the manual inflation of two tori attached to the top and bottom of PILLARS. Astronauts do not have to erect any rigid structures, as they might for other dust-mitigation systems. There is much less astronaut time needed for the continued operation of PILLARS since the system will expand and deflate on its own after initial setup.

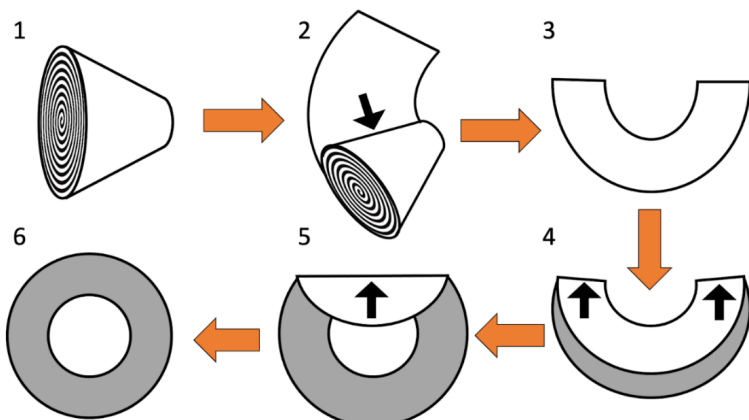


Figure 3-15: Deployment operation from rolled up stowed configuration to unrolled, flattened torus.



Figure 3-16: Inflated bladder structure. The bottom edge of the torus is

In terms of an anchoring system, we are currently speced to use the 1kg single helix anchors proven in the LATTICE system TRL 4. There is precedence in this design with the helical flute and rotary percussive design for the TRIDENT drill (Honeybee Robotics) set to fly in early 2025. The LATTICE team was able to get upwards of 2.5 kN of force on these anchors with no noticeable soil displacement and simulations indicate that the angular grains on the lunar surface would provide even better performance. Thus, anchoring capability is not a limiting factor of the design but there is room for future trade studies on the complexity of deployment and packaging the required anchors into a lander as opposed to utilizing stronger anchors such as the Manta Ray anchors that are rated for 10s of kN.

3.7 Risk Matrix

	Negligible	Minor	Moderate	Severe	ID	Risk	Mitigation	ID	Risk	Planned Mitigation/Testing
Frequent	MECH-02	ENV-02	MECH-03 MECH-04 MECH-09		MECH-01	PILLARS does not inflate in a way that contains the regolith	Simulation and Test	MECH-10	Off-centered landing could cause failure shear on the anchors	Simulation and Test, Margin
					MECH-02	Anchors cannot handle the stress from plume forces on PILLARS	Simulation and Test, add margin on ability to withstand force	MECH-11	Anchors and inflatable connection tears	Lifetime Testing
					MECH-04	PILLARS can deteriorate quickly due to the plume force and pressure	Lifetime Testing	ENV-01	Craters formed from the repeated landings can cause uneven surfaces	Analysis of compatibility with low-SWaP surface preparation systems
Likely		ENV-01	ENV-03 MECH-10		MECH-01	PILLARS can deteriorate quickly from the regolith abrasion	Lifetime Testing	ENV-02	UV, Temperature, and regolith environment could weaken the Kevlar mesh	System Lifetime Material Analysis using DSNE data
					MECH-06 MECH-11	PILLARS can become dislodged from its location	Add margin on force experienced by berm	ENV-03	Accumulated regolith from previous launches is accelerated by plume and impacts rocket	Simulation and Test
					MECH-07	PILLARS does not contain enough of the disturbed regolith	Simulation and Test	ENV-04	Anchors are dug out due to cratering	Simulation and Test
Unlikely			ENV-05	MECH-05 OP-01 MECH-01	MECH-01	PILLARS cannot unfold or deploy properly	Test	ENV-05	Regolith may build up in system that may result in undetected work to service system	Simulation and Test
				MECH-09		Long term effects of factors such as rocket chemicals on system are unknown	System Lifetime Material Analysis and estimation	OP-01	PILLARS is made for astronauts traversal autonomy, avoid traversing with personnel traverse	
						Initial thrust on take-off will eject some regolith before PILLARS can fully expand	Simulation and Test			
Very Unlikely										

Figure 3-17: Updated Risk Matrix

3.8 Value Compared to Landing Pads

Tradespace Analysis of Landing Infrastructure Noah

- Comparison of various proposed systems for large lander support
- Deploy cost calculated with the assumption of \$10000/kg (Starship)

System	Mass	Diameter	Deploy time	Deploy cost for 10 launches	Energy consumption	Landings sustained
PILLARS	<10,000 kg	40m	<1 day	\$10-100 million	Low	>10
LILL-E Pad	54,030 kg	100m	>10 days	~\$500 million	Low	1-2
Construction	16-72,000 kg	100m	~30 days	\$260-480 million	High	>10

Construction of one lunar habitat for 4 people: \$35 billion



Figure 3-18: Landing Pad Comparison tradestudy

4 Verification Testing

4.1 High-temperature Abrasion Lifecycle Testing

We designed a test setup to validate the performance of Kevlar 49 under high temperatures and abrasion. A motorized linear actuator drives a steel rod back and forth, and at the tip of this rod, silicon carbide—a hard, abrasive material—is affixed, allowing it to effectively abrade fabric samples placed within a furnace. The actuator's cyclical motion simulates repetitive wear, which is critical for understanding material performance under prolonged regolith abrasion.

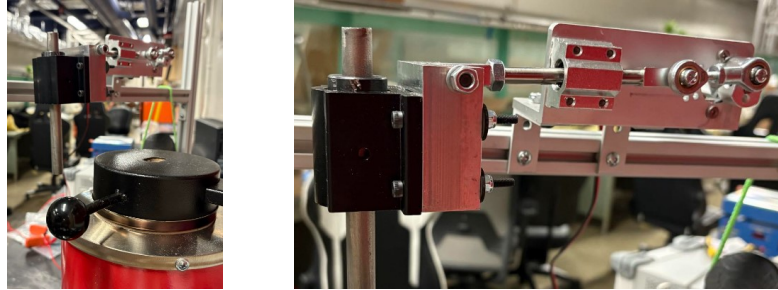


Figure 4-19: (a) The high-temperature abrasion test setup featuring a linearly actuated rod and a furnace; (b) The linear actuation mechanism designed to perform cyclical high-temperature abrasion testing.

Kevlar samples were subjected to approximately 5000 abrasion cycles at 300°C, 500°C, and 700°C. The amount of abrasion cycles was informed by the energy per unit area imparted on PILLARS by high-speed regolith. The energy per unit area was derived from the estimated volume of regolith displaced by a SpaceX Raptor engine, the average regolith grain size, and the average velocity of blasted regolith in the lunar atmosphere. An important observation from the abrasion testing is that none of the fabric samples were worn completely through, indicating a level of durability despite the high-temperature and abrasive conditions. The silicon carbide, while effective at creating surface wear, did not penetrate fully through any sample. The fact that minimal carbide particles were able to pass through the fabric layers highlights the material's capability to act as a barrier, when subjected to repeated abrasion.

4.2 Post-abrasion Tensile Testing

The tensile testing data gathered from the high-temperature abraded fabric samples provides insight into the material's structural integrity and its effectiveness in containing blasted regolith. By identifying the maximum force at which each sample begins to fray, we can assess the material's threshold for preventing structural degradation. This point of initial fraying is significant because it marks the beginning of fiber breakdown. Once fraying initiates, the fabric becomes susceptible to further tearing, and as fraying progresses, gaps form in the weave of the fabric, creating potential pathways for dust particles to escape.

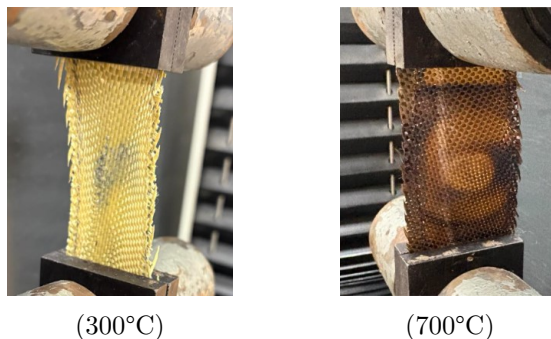


Figure 4-20: High-temperature abraded Kevlar samples prior to tensile testing.

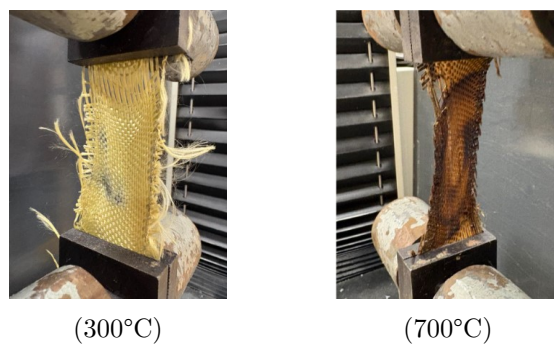


Figure 4-21: Fraying of high-temperature abraded Kevlar samples during tensile testing.

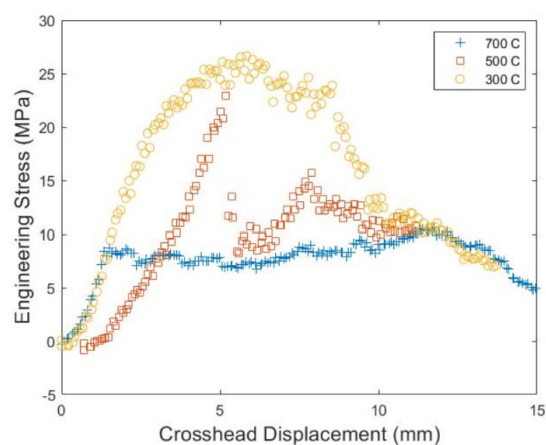


Figure 4-22: The stress-displacement curves of abraded Kevlar at varying temperatures.

Mean Tensile Stress at Fraying (MPa)	Temperature (°C)
26.6	300
22.9	500
10.6	700

Table 1: The mean tensile stresses at which fraying occurred in Kevlar samples subjected to high-temperatures and cyclical abrasion.

The tensile tests demonstrate that while Kevlar can tolerate moderate temperatures, such as 300°C before fraying, extreme temperatures (such as 700°C) severely impair its tensile strength and durability, resulting in fraying and inability to contain dust. Interestingly, the fact that fiber separation rather than a complete material breakdown occurred in both the 300°C and 700°C samples suggests that even at extreme temperatures, some level of fiber cohesion remains within Kevlar. This may indicate that while individual fibers have weakened and charred, the material retains some inherent cohesion, allowing the fibers to separate rather than disintegrate entirely. Furthermore, through testing, it is clear that the degradation of Kevlar is more heavily affected by high temperature than abrasion. Thus, while Kevlar may have the properties needed to withstand abrasion from regolith alone, it significantly degrades when subjected to high temperatures in tandem. Based on the observed degradation of Kevlar 49 at high temperatures, there is a clear indication that alternative materials with higher thermal resistance—such as ceramic fiber fabrics—would be better suited for applications that involve prolonged exposure to both abrasion and extreme temperatures.

4.3 Prototyping for Room Temperature Flows in Atmosphere and Vacuum Conditions

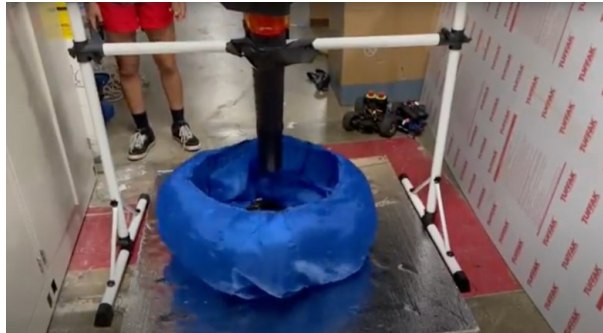


Figure 4-23: Leaf blower test stand for observing inflation behavior given different fabric densities, flow speeds, anchor configurations, and pattern shapes.

To understand the inflation dynamics of PILLARS, we started with the most basic proof of concept demonstration. In atmosphere with room temperature flow, a leaf blower was used to simulate a rocket plume impinging on a nylon prototype. The diameter of the model is 1/20 scale of the lunar PILLARS and the mass flow rate of the leaf blower is approximately 1/1300 the mass flow rate of a raptor engine. The scaling of mass flow rate and diameter is not perfect, so we opted for a material with a much lower tensile strength and stiffness than kevlar. This test stand was used to investigate the inflation dynamics of many different prototypes.

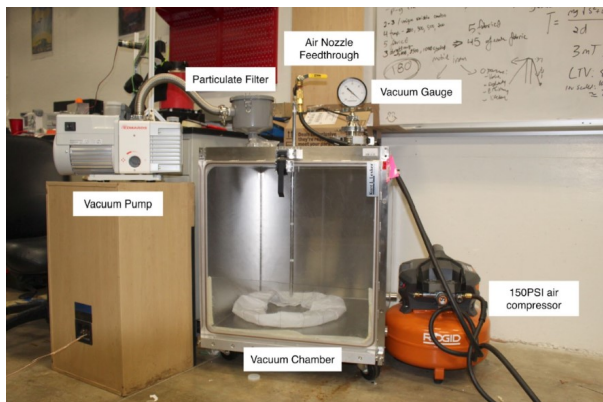


Figure 4-24: Vacuum system including 226L chamber, Edwards R5 vacuum pump, 150 PSI air compressor, 2 micron particulate filter, custom feedthrough for gas insertion, and vacuum gauge.

Due to differences in back pressure, the inflation mechanism of PILLARS in atmosphere is not characteristic of the inflation mechanism on the moon. To better understand the lunar inflation case, we purchased a 226L square vacuum chamber with an acrylic door for viewing. The air compressor has a maximum flow rate of 2.6 CFM, so we selected the Edwards Rotary Vane 5 vacuum pump with a peak pumping speed of 3.6 CFM to maintain vacuum during gas injection. The ultimate pressure is 10⁻³ Torr, which is sufficiently low for a vacuum chamber of this size. To perform gas injection, a custom feedthrough was made for a blow gun with extensions using a flange adapter and vacuum rated epoxy. This allows for the compressed air to be released manually only after the chamber achieves the desired pressure. A 2 micron particulate filter was installed between the pump and chamber to allow dust simulant testing without damaging the pump.

4.4 Hot Fire Testing in Atmosphere Conditions

Inflation tests performed with room temperature flows are fundamentally uncharacteristic of the inflation behavior with a high temperature flow. We initially intended to use model rocket engines with a small model to verify hot fire inflation, however, the short burn duration (order of 1s) and logistical challenge of safely igniting unpredictable rockets forced us to pursue a propane torch test stand instead. The test was much safer because the propane flow was easily regulated with a valve. The torch did not have enough pressure to inflate the models so the mechanism was not validated.



Figure 4-25: Hot fire test stand using 500,000 BTU/hr propane torch suspended over a cement plate with through holes for model mounting. The stand is wrapped in chicken wire to prevent burning material from blowing away.

4.5 Liquid Bi-Propellant Rocket Static Fire

Friends of Amateur Rocketry (FAR) is a rocket testing facility in the Mojave that serves many student rocket organizations around the country. Student teams are able to travel to the test site and safely test fire their rockets of all shapes and sizes. We tested PILLARS with a prototype liquid bi-propellant rocket developed by FAR as a kit for student teams.

Exit Nozzle Diameter	2.73 in
Throat Diameter	1.38 in
Fuel Composition	LOX + 50% Ethanol/50%Methanol
Maximum Thrust	500 lbf
Mass Flow Rate	2 lb/s
Chamber Temperature	5,250°F
Chamber Pressure	300 psi

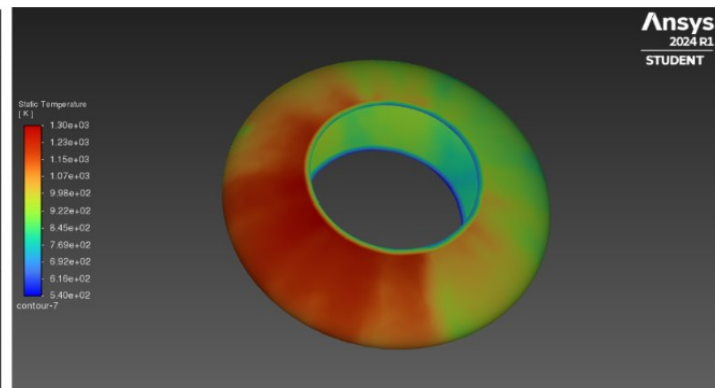


Figure 4-26: Rocket specifications for the FAR liquid bi-propellant rocket on the left, used to generate the 3D Ansys simulation on the right. Simulation was used to inform prototype design.

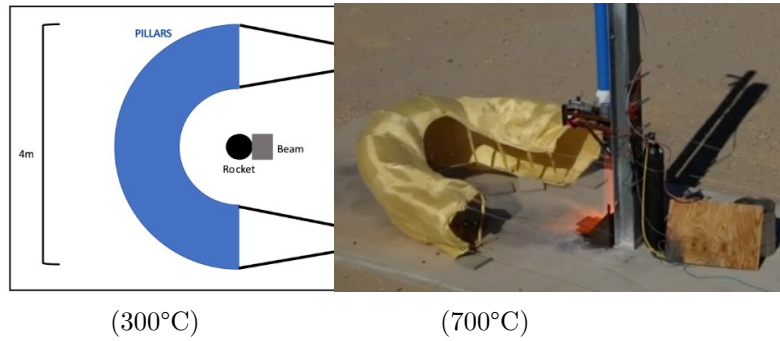


Figure 4-27: Diagram and photo of FAR test conducted on August 24, 2024. PILLARS is anchored to two points in the dirt behind the rocket launch pad with in-line load cells to measure tangent force and verify stresses in the shield. PILLARS inflated as expected before the ground anchors were blown away.

The 4m model tested at FAR on August 24th survived for a short time, but ultimately was destroyed over the course of the test. Due to the static fire mounting hardware blocking the plume, it was not possible to test a 360° model. Flaws in the anchor design resulted in invalid load cell data and failed to constrain vertical motion. Observation of the model post-fire revealed major insights about shield design construction, leading to a second prototype. Further testing is required to investigate the capability of the updated system due to rocket failure during the second test.



Figure 4-28: Photos from FAR test on October 21st, 2024. Pictured on the left is the PILLARS prototype anchored to metal struts secured on either side of the launch pad next to a failed rocket launch. On the right is the extensive damage done to the rocket motor by a valve failure in the LOX line.

5 Path to Flight

Rocket plume driven sand storms can damage landed infrastructure, reduce the effectiveness of solar panels and radiators as well as coat optics. This dust can travel many times around the moon with each event. As the reach is global on the moon, mitigation is a prerequisite for a working sustainable presence.

In order to establish a lunar base and jumpstart NASA's desire for a robust lunar economy, there will be a frequent cadence of landings on the Lunar South Pole. Current mobility systems for offloading the lander and transportation are primarily being studied to support transport within 5km of the landing site. In order for such ranges to be possible, it is a necessity that the abrasive dust is mitigated on landing.

Without significant pre-existing infrastructure, PILLARS fills the initial gap of plume diverting berms. Being able to have many more easily placed on the surface, reduces the required distance to travel from the landing sites to the mobile habitats, and protects the landed assets. Moreover, multiple sizes for CLPS, Starship HLS, Blue Moon, supports having a tailororable solution that can be pre deployed and moved to accommodate future missions gives this technology an edge over the large initial investments in less rapid solutions. Having a versatile and scalable solution is very desirable while the long term locations and infrastructure is finalized.

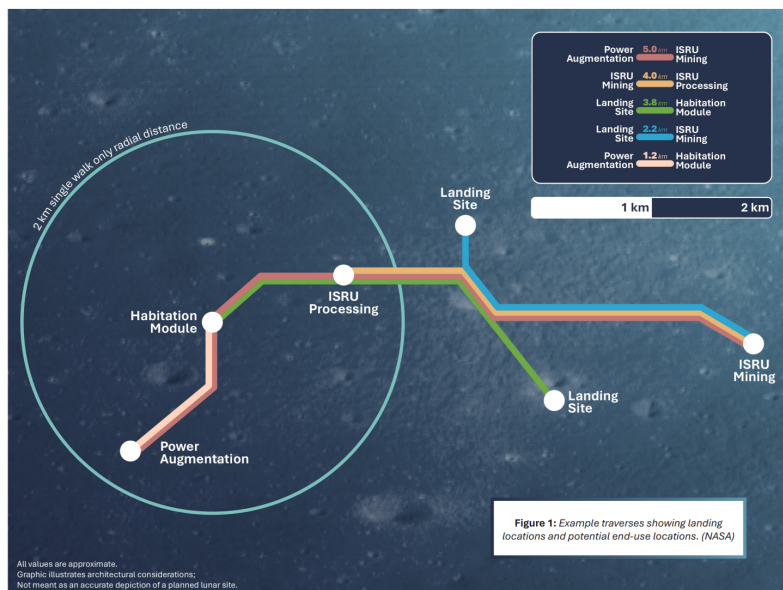


Figure 5-29: Notional lunar base functionalities and locations from the NASA Moon to Mars mobility drivers whitepaper.

System Component	Start TRL	Advancement Plan	End TRL
Inflatable Material	3	Abrasion Test, Pressure + Temp Test	5
Rocket Inflation	2-3	CFD, Scaled down plume vacuum testing	4
Anchoring System	3	Anchor Testing	4
Berm for Dust Mitigation	3	CFD, Scaled down plume vacuum	4
Inflatable Deployment	3	Scale deployment test	4

Figure 5-30: Table mapping TRL maturation for components of PILLARS.

At the end of the BIG Idea Challenge, we have verified breadboard PILLARS components in a laboratory environment in addition to preliminary simulations of the interactions between the plume and inflatable berm. With that, we claim that the system is at TRL 4. In order to

scale this system to support the needs for large-scale lunar landing, we believe there are viable paths to validate the gaps in the system development which shall be elaborated upon in the following section.

In order to validate this system to TRL 5 we need to be able to test a brassboard in relevant analog conditions. This means validating the survivability, deployment, and mitigation capabilities of the full system. We currently have a brassboard prototype completed to conduct relevant tests on survivability and deployment. To complement these tests, there are still additional simulation capabilities that are to be desired in order to determine analog conditions and projected dust mitigation capabilities. With the added simulation capability and this prototype, we seek to do a test of a scaled-down prototype at the FAR facility to validate survivability in the harsh plume conditions. The FAR test combined with the existing abrasion testing should provide verification that the system can withstand the landing conditions. This prototype can also be used to validate scaled down autonomous deployment of the anchoring system to ensure that the current deployment strategy is viable. Lastly, a smaller version of this system will need to be utilized to verify the dust mitigation capabilities in a relevant environment. There exists various platforms to conduct these tests from Astrobotic’s Floatatinator test stand that can provide gravity offloaded Plume Surface Interactions or the existing dirty vacuum chamber setup that was developed for this test.

Achieving TRL 6 requires that the at-scale prototype is developed and rigorously verified in relevant conditions. Such tests would require a significant partnership with existing lander companies to provide the scale needed for verification. Potential paths forward include working with Blue Origin’s current BE-7 test planning at the Edwards Airforce Base thermal vacuum chambers, deploying a technology demonstrator off of a CLPS lander and testing with a representative hopper, and deploying a scaled-down system off of a representative lander such as Blue Origin’s Mark 1 lander and recording SCALPSS data during landing and takeoff. In any case, extensive collaboration is required with a lander company to not only integrate an at-scale test but to also determine critical interface requirements for the overall system. Due to the versatility of PILLARS, the various testing options highlight the fact that it is significantly easier to deploy an at-scale system as a “rideshare” or add-on to the mission which can help increase the likelihood of maturation through TRL 6.

Once at TRL 6, the full system will be ready for deployment and operation within NASA’s Moon to Matrs architecture. In collaboration with a commercial landing company, the PILLARS system will be delivered to the surface at the desired landing site. Utilizing the mobility and logistics capabilities that are currently being developed through initiatives such as the NextSTEP-R-2, the system will be offloaded and deployed concurrently with robotic services such as those being developed by Gitai. Once these systems are established, it will be able to continually protect the growing lunar settlement for future launches and landings.

6 Project Management

6.1 Leadership and Management

Our team is split into seven subteams: (1) Simulation, (2) Materials, (3) Deployment, (4) Prototyping, (5) System Integration, (6) Project Management, and (7) Mission Concept. The Simulation subteam is responsible for fluid, temperature, and pressure and structural analysis of our system and prototyping design. The Materials subteam is responsible for assessing the properties of materials used in our inflatable and fabrication methods. The testing subteam is responsible for the testing setups and result analysis. The Deployment subteam is responsible for the anchoring mechanism of the inflatable. The Prototyping subteam is responsible for making the prototypes and evaluating the design. The System Integration subteam is focused on conceptual design and integration of information from the other four subteams in addition to developing and implementing a testing scheme. Communication among all team members is facilitated through online communications as well as weekly team meetings on mondays to discuss updates from last week and assign deliverables for the coming week to maintain awareness of the whole project and accountability for individual deliverables.

The team schedule is based on the Agile method of project management. In a week, the team meets once for a long work session, once for a short tag-up session led by the leadership team, and once for a short subteam tag-up with the respective lead. Additional unofficial work sessions are organized alongside individual work and research time. To ensure steady progress, one to four-week sprints were set, each closed with a technical review, where the team received valuable feedback from experts in aerospace engineering. During these reviews, major decisions have been made following the feedback of experts. Most work was completed by sixteen students working on campus during the summer period. Through various programs on campus, students were funded for their work over the summer as described later in the budget section, contributing to the success of PILLARS.

Crucial to our continued success, we have been able to enlist the support and advice from several renowned experts in the field of aeronautics and space engineering. Kalind Carpenter, a Robotics Mechanical Engineer at JPL, has been integral to the development of this project. We have received continued support from our advisor, Dr. Charles Elachi. His experience as the former director of JPL for 16 years, Professor Emeritus in Electrical Engineering and Planetary Science at Caltech, and project lead for countless space science missions position him as an invaluable advisor to evaluate the scientific and engineering credibility of PILLARS. To hold the team accountable for progress, we have met with these advisors once a month or more as needed throughout development. Finally, Dr. Soon-Jo Chung, a Bren Professor of Aerospace and Jet Propulsion Laboratory Research Scientist, has played a critical role as our primary advisor with weekly meetings. We have also formed various partnerships to help develop PILLARS. One such partnership is with Cislune, a lunar construction and ISRU company. We also partnered with Friends of Amateur Rocketry, allowing us access to a rocket test stand.. Finally, we have partnered with Dr. Joe Shepherd in the Caltech Explosion Dynamics Lab to access a thermal vacuum chamber for testing material properties for the inflatable. Dr. Shepherd has been an invaluable source of support for both facilities and expertise on the PILLARS project.

6.2 Project Schedule

Throughout work on PILLARS, we have found that the timeline of work completed was much less consistent than initially expected. Rather than continual steady progress, PILLARS experienced a project lifetime of stalled progress followed by very rapid bursts of development. This is due to many factors, but was mainly governed by personnel availability, especially as students leave campus around the beginning and end of the summer period, closely aligning with deadlines for the midterm and fall status reports. Our clearest critical path was our path to testing at Friends of Amateur Rocketry, as this required development on simulations to govern the shape and size of the berm, which would then govern prototyping efforts before testing at FAR. Though we stayed mostly on track, one major hindrance to this critical path was a fire in the building housing our on-campus lab space within the week of our final FAR test. With access lost to the building for nearly a week and still no access to an elevator to move our components to and from lab, we were greatly hindered in our ability to conduct field testing. However, we were still able to successfully finish testing PILLARS in spite of this delay.

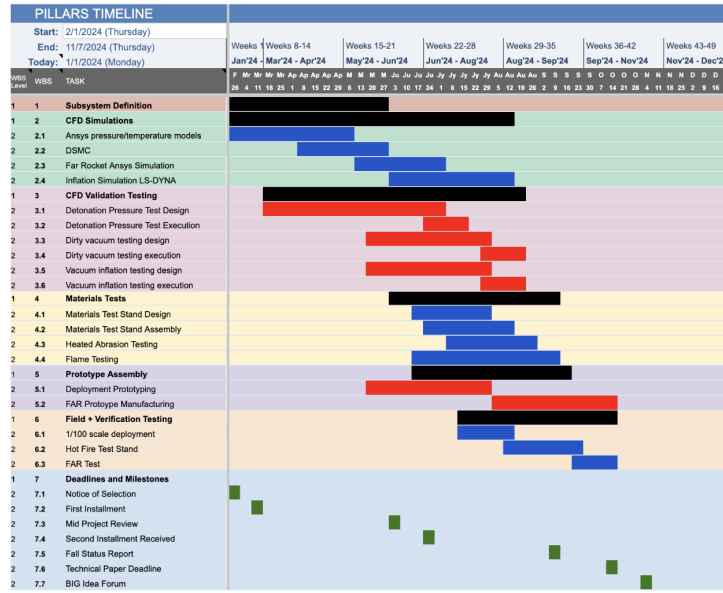


Figure 6-31: Updated Gantt Chart for our Development.

6.3 Budget

6.3.1 Direct Labor

Advisors

Dr. Soon-Jo Chung was responsible for project coordination and supervision of undergraduate students and project personnel. Mr. Kalind Carpenter assisted with project coordination, and is affiliated with the NASA Jet Propulsion Laboratory. Neither of these individuals were compensated for their advisory role.

Summer Labor Seven undergraduate students participated in Caltech's SURF program during the summer of 2024. These positions were 10 weeks long, and were officially mentored by Dr. Soon-Jo Chung. These appointments were dedicated to a mix of prototyping, materials testing, and simulations. Students received a stipend of \$7,740 for the entire period, but half of this stipend (\$3,870) was funded by the SURF Office. This left us responsible for \$27,090. We extended the SURFs for an additional 3 weeks for all students, for which we paid \$2,322 per student. Alongside the SURF program, we paid two additional students for 10 weeks of work at the SURF rate. For these students, we fronted the entire \$7,740 cost, adding an additional \$15,480. All told, we paid \$58,824 for student labor over the summer, proving to be an effective way of keeping the team involved over the summer.

Alongside the paid labor, we were also fortunate to take on students fully funded by Caltech. Through the WAVE Fellows program, we were able to take on two students from underrepresented backgrounds who were fully funded by Caltech for a stipend of \$6,000. Also, the First-year Success Research Institute (FSRI) Program enabled us to take on three incoming first-year undergrads, who joined the PILLARS team at the end of the summer, prior to their first year at Caltech. These students were also entirely funded by Caltech, and worked at no cost to us.

6.3.2 Equipment and Testing

Much of the equipment purchased for this project was used for testing and manufacturing. For manufacturing equipment, we bought 5 heavy duty sewing machines for \$300 each and an industrial sewing machine for \$2,000, totaling \$3,500 spent on prototyping equipment. We were also able to buy a small-scale vacuum chamber for \$8,000 for small in-house dirty vacuum testing. Alongside this, we spent \$15,000 constructing a testing apparatus to use within the Caltech Explosion Dynamics Laboratory thermal vacuum chamber. For testing materials properties, we also purchased 2 small furnaces at \$200 each. For machining parts for the materials testing assembly, we spent an additional \$5,000. Our only contracted test at FAR, which happened twice, cost us about \$1,500 per run, totaling \$3,000.

6.3.3 Materials

For materials testing, we purchased very large quantities of Kevlar and Carbon Fiber felt rolls for the scale models for rocket testing at FAR. To help us prototype with these materials, we purchased kevlar thread and anti-fray adhesive. Alongside these materials, we also purchased a Carbon-Kevlar hybrid and silicon carbide lapping grains to aid in materials testing. The total cost for materials to test was \$8,060.

6.3.4 Travel

As we are now traveling to Las Vegas, we are opting to drive from Los Angeles to Las Vegas. We were able to apply to Caltech's George W. Housner fund, providing \$6,380 to cover hotels and transportation to the BIG Idea Forum. As such, we pay only the registration fees for the BIG Idea Forum and LSIC Conference, totaling \$6,530.

6.3.5 Indirect Costs

For Caltech, the indirect cost is calculated at 25% of total direct costs (or 20% of total cost). The reduced indirect cost rate of 25% total direct costs is applied by special approval from the Caltech Provost. For the California Space Grant Consortium, the indirect cost is calculated at 48.5% of total modified direct costs, which only includes the first \$25,000 of the subaward that will be issued to the California Institute of Technology. The total indirect cost paid is \$39,700.

Personnel Costs [A]	Cost Per	Qty	Total	Travel Costs [D]	Cost Per	Qty	Total
SURF Summer Students	\$3,870	7	\$27,090	Hotel Room (3 bed/2 nights)	\$719	5	\$3,595
Extended SURF Appointments	\$2,322	7	\$16,254	Hotel Room (3 bed/3 nights)	\$1,079	2	\$2,158
Additional Student Researchers	\$7,740	2	\$15,480	Gas (per gallon)	\$4.60	600 miles 5 cars 22mpg	\$627
			TOTAL: \$58,824	BIG Idea Forum Registration	\$250	21	\$5,250
Equipment & Testing Costs [B]	Cost Per	Qty	Total	LSIC Registration	\$80	16	\$1,280
Heavy Duty Sewing Machines	\$300	5	\$1,500				TOTAL: \$12,910
Industrial Sewing Machine	\$2,000	1	\$2,000				HOUSNER: \$6,380
Dirty Vacuum Chamber	\$8,000	1	\$8,000				PILLARS: \$6,530
Testing Apparatus for TVAC	\$15,000	1	\$15,000	Materials Costs [C]	Cost Per	Qty	Total
Furnace for Materials Testing	\$200	2	\$400	Kevlar 49 Roll	\$50	70	\$3,500
Materials Testing Parts	\$5,000	1	\$5,000	Carbon Fiber Felt Roll	\$50	40	\$2,000
FAR Rocket Test	\$1,500	2	\$3,000	Carbon-Kevlar Hybrid Roll	\$80	2	\$160
			TOTAL: \$34,900	Silicon Carbide Lapping Grains	\$80	1	\$80
Indirect Costs [E]	Rate		Total	Kevlar Thread Spool	\$50	40	\$2,000
Caltech Phase 1	25% on direct costs		\$15,000	Anti-Fray Adhesive	\$8	40	\$320
Caltech Phase 2	25% on direct costs		\$12,575				TOTAL: \$8,060
CASGC Phase 2	48.5% on first \$12k of direct costs		\$12,125				
			TOTAL: \$39,700				

Figure 6-32: Detailed spending by sub-group listed above.

Category	Phase 1	Phase 2	Total
[A] Personnel	\$0	\$58,824	\$58,824
[B] Equipment	\$31,900	\$3,000	\$34,900
[C] Materials	\$8,060	\$0	\$8,060
[D] Travel	\$0	\$6,530	\$6,530
[E] Indirect Cost	\$15,000	\$24,700	\$39,700
Total	\$54,960	\$93,054	\$148,014

Figure 6-33: Total spending broken down by phase. Note that the entire summer period falls in phase 2, so all of our paid labor accordingly makes phase 2 much more expensive than phase 1.

References

- [1] Bob Esser et al. *The Path to an Enduring Lunar Presence*. 2023. URL: <https://lsic.jhuapl.edu/Resources/files/The%20Path%20to%20an%20Enduring%20Lunar%20Presence.pdf>.
- [2] Christopher Immer et al. “Apollo 12 Lunar Module exhaust plume impingement on Lunar Surveyor III”. In: *Icarus* 211.2 (2011), pp. 1089–1102. ISSN: 0019-1035. DOI: <https://doi.org/10.1016/j.icarus.2010.11.013>. URL: <https://www.sciencedirect.com/science/article/pii/S001910351000432X>.
- [3] Matthew Kuhns et al. “Instant Landing Pads for Lunar Missions”. In: *Earth and Space 2021*, pp. 1027–1032. DOI: [10.1061/9780784483374.094](https://doi.org/10.1061/9780784483374.094). eprint: <https://ascelibrary.org/doi/pdf/10.1061/9780784483374.094>. URL: <https://ascelibrary.org/doi/abs/10.1061/9780784483374.094>.
- [4] John E. Lane and Philip T. Metzger. “Estimation of Apollo Lunar Dust Transport using Optical Extinction Measurements”. In: *Acta Geophysica* 63.2 (2015), pp. 568–599. ISSN: 1895-7455. DOI: [10.1515/acgeo-2015-0005](https://doi.org/10.1515/acgeo-2015-0005). URL: <https://doi.org/10.1515/acgeo-2015-0005>.
- [5] Philip T. Metzger and Greg W. Autry. “The Cost of Lunar Landing Pads with a Trade Study of Construction Methods”. In: *New Space* 11.2 (2023), pp. 94–123. DOI: [10.1089/space.2022.0015](https://doi.org/10.1089/space.2022.0015). eprint: <https://doi.org/10.1089/space.2022.0015>. URL: <https://doi.org/10.1089/space.2022.0015>.
- [6] NASA. *BIG Idea Challenge 2024 Proposal Guidelines*. 2023. URL: <https://bigidea.nianet.org/wp-content/uploads/2024-BIG-Idea-Challenge-Proposal-Guidelines.pdf>.
- [7] NASA. *NASA Moon to Mars Architecture Definition Document*. NASA/TP-20230017458. Washington, DC, USA, 2024. URL: <https://www.nasa.gov/wp-content/uploads/2024/01/rev-a-acr23-esdmd-001-m2madd.pdf?emrc=65bc346d13714>.
- [8] NASA *Lunar Surface Innovation Initiative*. 2024. URL: <https://www.nasa.gov/space-technology-mission-directorate/lunar-surface-innovation-initiative/>.
- [9] Michael Pohlen et al. “Overview of lunar dust toxicity risk”. In: *npj Microgravity* 8.1 (2022), p. 55. ISSN: 2373-8065. DOI: [10.1038/s41526-022-00244-1](https://doi.org/10.1038/s41526-022-00244-1). URL: <https://doi.org/10.1038/s41526-022-00244-1>.
- [10] TRAVIS VAZANSKY et al. *LUNAR IN-SITU LANDING/LAUNCH ENVIRONMENT (LILL-E) PAD*. 2021. URL: <https://bigidea.nianet.org/wp-content/uploads/Colorado-School-of-Mines-Final-Technical-Paper-2021-BIG-Idea.pdf>.